TRENDS IN SCIENCES 2025; 22(9): 10194
https://doi.org/10.48048/tis.2025.10194
RESEARCH ARTICLE

Design and Evaluation of Mn(II) Cysteine-Alanine Dithiocarbamate Complexes: Insights from Molecular Docking and Cytotoxicity Against MCF-7 Breast Cancer Cells

Andi Besse Khaerunisa[1], Indah Raya[1,*], Hasnah Natsir[1], Nunuk Hariani Soekamto[1], Abdul Wahid Wahab[1], Rugaiyah Arfah[1], Rizal Irfandi[2], Eka Pratiwi[1], Wahyudin Rauf[1] and Andi Adillah Nur Syafirah[3]

[1]Department of Chemistry, Faculty of Mathematics and Natural Science, Hasanuddin University, Makassar 90245, Indonesia
[2]Department of Chemistry, Faculty of Mathematics and Natural Science, Universitas Negeri Makassar, Makassar 90244, Indonesia
[3]Department of Internal Medicine, Faculty of Medicine, Hasanuddin University, Makassar 90245, Indonesia

([*]Corresponding author's e-mail: indahraya@unhas.ac.id)

Received: 18 March 2025, Revised: 20 April 2025, Accepted: 27 April 2025, Published: 1 July 2025

Abstract

This study aims to synthesize, characterize, and evaluate the anticancer potential of a manganese(II) cysteine-alanine dithiocarbamate complex to overcome challenges posed by drug resistance in breast cancer treatment. The Mn(II) cysteine-alanine dithiocarbamate complex was synthesized using manganese chloride, alanine, cysteine, and carbon disulfide under controlled conditions. The synthesized complex exhibited strong thermal stability (melting point: 200 – 218 °C) and weak electrolyte behavior (conductivity: 1.5 mS/cm at 28 °C). Characterization techniques included UV-Vis (absorption peaks at 253, 274, 284, 294, and 305 nm), FTIR (notable bands at 3338.78, 2918.30, 1597.06 and 689.30 cm^{-1}), XRD (sharp peaks at 28°, 32°, 43°, 60°, lattice parameters a = 3.40 Å, b = 2.48 Å), and SEM-EDS (porous morphology with dominant Mn and S content). Molecular docking revealed strong interactions with estrogen receptor alpha (ERα) through hydrogen bonds, van der Waals forces, and salt bridges, with a binding energy of −59.93 kJ/mol. Cytotoxicity was evaluated on MCF-7 cells using the MTS assay, revealing a dose-dependent inhibition with an IC_{50} value of 61.66 µg/mL. The Mn(II) cysteine-alanine dithiocarbamate complex exhibits promising structural stability, receptor binding affinity, and cytotoxic potential against MCF-7 breast cancer cells, highlighting its potential as an effective and selective anticancer agent.

Keywords: Complex, Breast cancer, MCF-7 cell lines, IC_{50}

Introduction

Breast cancer ranks among the foremost causes of cancer-related mortality in women globally, with an estimated mortality rate exceeding 400,000 per year [1]. Although cancer therapies have advanced in various ways, including chemotherapy, targeted therapy, and immunotherapy, a major challenge remains in drug resistance [2]. This resistance, which can appear at the onset or develop throughout treatment, represents a significant barrier in breast cancer treatment, especially in advanced stages or when the cancer has metastasized [3]. This resistance reduces the effectiveness of treatment, often causing relapse and worsening the patient's condition, resulting in a lower survival rate [4]. Research indicates that drug resistance in breast cancer involves complex mechanisms, including changes in the tumour microenvironment and metabolic adaptations in cancer cells, which enable these cells to withstand the effects of anticancer therapies [5]. This highlights the

urgent need to identify alternative, more effective and safer alternative therapies.

In recent decades, research on metal complexes has identified the potential of metal-based anticancer agents, such as platinum, palladium, and other complexes, which may combat breast cancer, including drug-resistant variants [6]. However, the clinical use of platinum metals is often hampered by toxic effects and emerging resistance, creating a need for alternative metals, such as gold, nickel, and manganese, which exhibit selective cytotoxicity toward cancer cells [7]. Manganese (Mn), in particular, has attracted attention in anticancer research because it can generate reactive oxygen species (ROS) that disrupt mitochondrial activity, induce DNA damage, and lead to cancer cell death through intrinsic pathways [8]. Research by Yadamani *et al.* [9] indicated that the cytotoxic effects of Mn (III) complexes are enhanced at elevated concentrations and extended treatment durations, with an IC_{50} value for Mn (III) complexes on MCF-7 cells determined to be 2.5 mmol/L following 24 h of treatment. Additionally, Mn(II) complexes derived from Schiff base made from pyridoxal have shown cytotoxic effects on breast cancer cells and have been able to induce apoptosis, as confirmed by flow cytometry [9].

The synthesis of metal complexes involves reactions between transition metals and organic ligands, which can stabilize the metal and influence molecular interactions within cells [10]. Using ligands such as dithiocarbamate can potentially strengthen interactions with biomolecules due to its chemical properties, allowing it to form stable complexes and induce redox shifts within cancer cells [11]. Structural characterization through techniques such as spectroscopy, crystallography, and *in silico* analysis is essential for verifying the composition and cytotoxic potential of the resulting complexes.

Molecular modelling approaches are also valuable for understanding the molecular interactions of Mn(II) complexes with target biomolecules. Through this research, we can observe how the structure of metal complexes affects their interactions with DNA and proteins, which contributes to their anticancer activity [12]. This modelling technique can further analyze the relationship between molecular structure and biological activity, allowing for structural modifications that enhance anticancer activity while reducing toxicity [13].

The multidisciplinary approach, encompassing synthesis, characterization, and molecular modelling of Mn(II) complexes, is expected to provide new insights for developing more selective and effective metal-based cancer therapies. If proven successful, Mn(II) cysteine-alanine dithiocarbamate complexes have the potential to become efficient therapeutic agents, offering an alternative for cancer therapy with fewer side effects.

Materials and methods

Every chemical and reagent (perovskite analytical) acquired was of expert quality. The components obtained from the Central Laboratories of Hasanuddin University and Padjadjaran University, Indonesia, consist of Zinc(II) Chloride, Cisplatin, Alanine, Cysteine, Carbon Disulfide (CS_2), Potassium Hydroxide (KOH), Parafilm, Aquabides, Dimethyl Sulfoxide (DMSO), Potassium Bromide (KBr), and 95% Ethanol.

Targeting proteins in breast cancer cells through molecular docking of complex compounds.

The YASARA software was employed to prepare the protein and ligand for molecular docking. During this process, non-essential protein segments, cofactors, and superfluous ligands were eliminated. The ligand was synthesized in MarvinSketch at pH 7.4 and saved as ligand_2D.mrv. The “Conformers search” feature was employed to generate multiple ligand conformations in MarvinSketch, and the resulting files were saved as ligand.mol2. The ligand_2D.mrv file was reopened. The protein and ligand were docked using PLANTS, with protein.mol2 and ligand.mol2 serving as input files. The ligand's original position within the target protein structure was closely approximated by the docking pose with the highest score. Following the execution of these poses, RMSD (Root Mean Square Deviation) calculations are performed using YASARA. The technique is deemed valid if the moored position has an RMSD value of less than 2 Å (1 Å = 10 - 10 m) [14].

Synthesis of Mn(II) cysteine-alanine dithiocarbamate

For this synthesis, 0.2804 g of KOH was dissolved in distilled water, followed by the dropwise addition of 0.302 mL of CS_2 (5 mmol) into 10 mL of ethanol at 10 °C. Next, 0.445 g of alanine was added and stirred in the

mixture for 25 min. Subsequently, 0.6058 g of cysteine was introduced, followed by 0.622 g of $MnCl_2$ dissolved in 10 mL of ethanol. The solution was stirred using a magnetic stirrer for 30 min, filtered and dried, and recrystallized the resulting precipitate. **Figure 1** illustrates the synthetic route for Mn(II) cysteine-alanine dithiocarbamate.

UV-Vis absorption spectrofotoscopy

The Mn(II) cysteine-alanine dithiocarbamate complex was solubilized in ethanol at a concentration of 100 ppm. The electronic spectrum from 200 to 400 nm was subsequently analyzed via a UV-Vis spectrophotometer.

Characterization with fourier transform infrared spectroscopic

The Mn(II) cysteine-alanine dithiocarbamate complex was compressed into a pellet using dry Potassium Bromide (KBr) and subsequently analyzed via FT-IR spectroscopy within the wavenumber range of 340 - 4000 cm^{-1}.

Characterization with x-ray diffraction (XRD)

We validated the crystal morphology using an XRD-7000 Shimadzu Maxima at −90 °, taking measurements in increments of 0.02 ° per step. The resultant diffractogram was acquired, illustrating peak strength (counts) in relation to the diffraction angle (2θ).

Characterization with scanning electron microscopy (SEM)

We performed an analysis using a Scanning Electron Microscope (SEM) with the JEOL JCM 6000plus. We affixed the specimen to a block stage with a carbon tip and adjusted it with an electric blower. We then positioned it in a preparation box within the stage holder for coating. The stage holder bolts were tightened with an “L” key, and the SEM was employed to analyze the morphology of the Mn(II) cysteine-alanine dithiocarbamate complex.

Characterization using scanning electron microscopy with energy dispersive spectroscopy

Following SEM analysis, the Mn(II) cysteine-alanine dithiocarbamate complex was further examined using SEM-EDS at a specific site on the sample. The sample's surface emitted X-rays, which were detected by an Energy Dispersive Spectroscopy (EDS) detector to determine its elemental composition.

Anticancer activity test against breast cancer cells

The cytotoxic activity of the synthesized compounds was evaluated against MCF-7 breast cancer cells using the PrestoBlue™ cell viability assay. Complete RPMI-1640 medium supplemented with 10% fetal bovine serum (FBS) and 1% antibiotic was used for cell culture. Cisplatin was the positive control, and 2% Dimethyl Sulfoxide (DMSO) was used as the negative control. The test compounds were dissolved in a non-toxic solvent and diluted to the desired concentrations to prepare the working solutions.

MCF-7 cells with a minimum confluency of 70% were harvested using Trypsin-EDTA, centrifuged, and resuspended in a fresh medium. Cell viability and density were assessed via the trypan blue exclusion method, and cells were seeded at a density of 17,000 cells/well into 96-well plates. Plates were incubated at 37 °C with 5% CO_2 for 24 h for cell attachment.

Following incubation, cells were treated with serial dilutions of the test compounds, positive control, and negative control in duplicate and incubated for another 24 h under the same conditions. After treatment, 100 µL of a mixture containing PrestoBlue™ reagent (10% in culture medium) was added to each well and incubated for 1 - 2 h. The absorbance was then measured at 570 nm with a reference wavelength of 600 nm using a Thermo Fisher Scientific multimode reader. The percentage of cell viability was calculated to assess cytotoxic effects.

Results and discussion

The Mn(II) cysteine-alanine dithiocarbamate complex has a melting point of 200 - 218 °C, indicating good thermal stability. The thermal stability is similar to what was seen with similar complexes, like Mn(II) cysteine-alanine dithiocarbamate, which had a melting point of 204 - 206 °C. This shows that the interaction between the Mn(II) metal ions and the organic ligands makes the compound resistant to thermal breakdown [15]. Additionally, the electrical conductivity of the Mn(II) cysteine-alanine dithiocarbamate complex is 1.5 mS/cm at 28 °C, indicating that this complex behaves as

a weak electrolyte. This characteristic is ascribed to the robust contact between metal ions and organic ligands, which constrains ionic dissociation in solution. The findings can be compared to research on the Mn(II) proline-dithiocarbamate complex, which has a lower electrical conductivity of 0.3 mS/cm, which means it is not electrolytic [16]

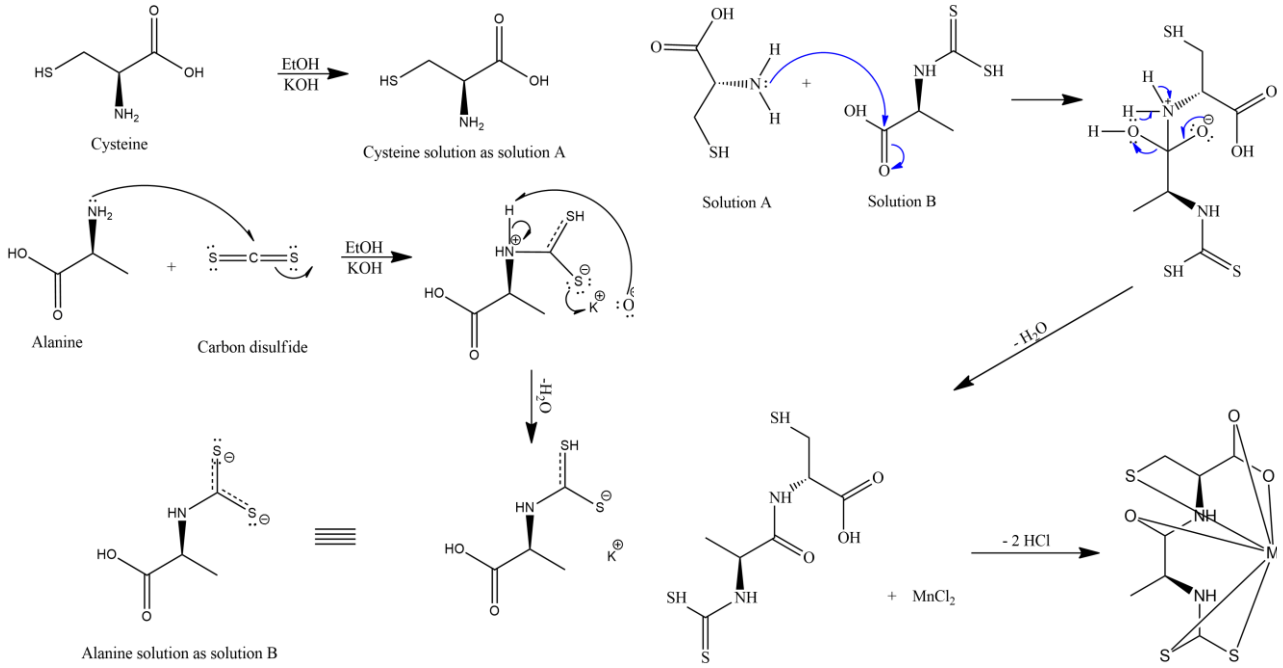

Figure 1 Synthetic scheme illustrating the formation of Mn(II) Cysteine-Alanine Dithiocarbamate complex through stepwise reaction of $MnCl_2$ with dithiocarbamate ligands derived from cysteine and alanine, highlighting the nucleophilic addition and coordination sites that lead to metal complexation.

Synthesis of Mn(II)cysteine-alaninedithiocarbamate

Molecular docking of complex on estrogen α

In contrast, the visualization of the control molecule 4,4',4"-[(2R)-butane-1,1,2-triyl]triphenol with estrogen receptor alpha (ERα) (**Figure 2**) demonstrates a different interaction pattern. In the control, interactions such as Pi-alkyl, alkyl, and Amide-Pi stacked are more prominent compared to the Mn(II) complex. Conventional hydrogen bonds are still present, as seen with the residue Trp (A:383), but they are fewer in number compared to the complex. Moreover, residues such as Ile (A:389) and Leu (A:511) mainly contribute through van der Waals interactions, with no significant contribution to stabilization as observed in the Mn(II) complex. The binding energy for the interaction of 4,4',4"-[(2R)-butane-1,1,2-triyl] triphenol with ERα is calculated to be −103.936 kJ/mol.

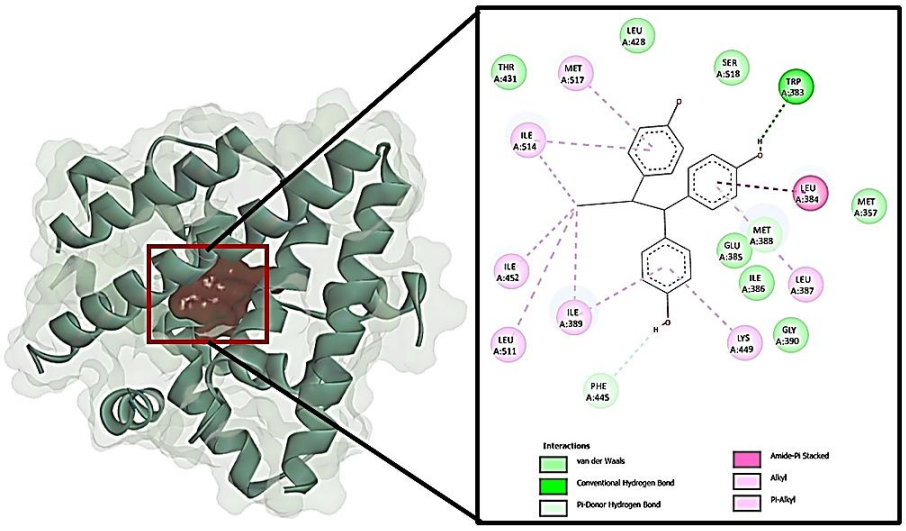

Figure 2 Molecular docking visualization of the positive control 4,4',4"-[(2R)-butane-1,1,2-triyl]triphenol with Estrogen Receptor α (ERα), showing key interaction types (e.g., Pi-alkyl, alkyl, and amide-Pi stacking) that contribute to moderate binding affinity.

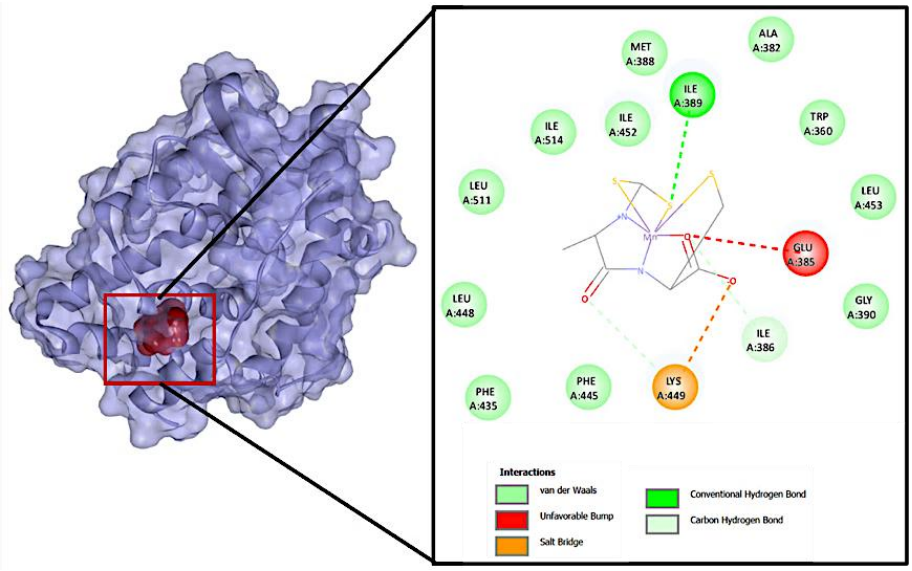

Figure 3 Molecular docking visualization of the Mn(II) Cys-Ala Dithiocarbamate complex with ERα, demonstrating key stabilizing interactions (e.g., hydrogen bonds, van der Waals forces, salt bridges) and highlighting the binding conformation at the active site.

The visualization of the interaction between the Mn(II) Cys-Ala DTC complex and estrogen receptor alpha (ERα) (**Figure 3**) reveals the presence of various types of interactions, including van der Waals forces, conventional hydrogen bonds, salt bridges, and carbon-hydrogen bonds. In this complex, the amino acid residues Glu (A:385) and Lys (A:449) appear to form specific interactions, such as salt bridges and hydrogen bonds, which play a significant role in stabilizing the complex at the active site of the protein [17]. Additionally, van der Waals interactions are predominantly observed with residues such as Ile (A:389), Met (A:388), and Phe (A:445), indicating the stability of the complex at the active site of the protein. The binding energy for the interaction between the Mn(II) Cys-Ala DTC complex and ERα is calculated to be −59.9348 kJ/mol.

To evaluate the binding energy of the Mn(II) Cys-Ala DTC complex, a comparison was made with compounds clinically utilized as ERα modulators. Tamoxifen, a selective estrogen receptor modulator (SERM) for breast cancer, shows a binding energy of approximately −3 kcal/mol or −12.55 kJ/mol against Erα [18]. This value is smaller in absolute terms than the Mn(II) Cys-Ala DTC complex, suggesting that the Mn(II) complex may have a stronger binding affinity. Conversely, natural compounds such as estriol, estradiol, and exhibit higher ERα binding affinities, with interaction energies of −418.9, −370.3 and −400.8 kJ/mol, respectively [19]. These values indicate that natural ligands exhibit a significantly higher affinity for the estrogen receptor than the Mn(II) complex. However, it is important to note that binding affinity is not the sole factor determining pharmacological effectiveness. Consequently, further studies—both *in vitro* and *in vivo*—are crucial to confirm the pharmacological potential of this complex.

UV-Vis characterization

Based on **Figure 4**, The peak at 253 nm is most likely attributed to electronic transitions in the chromophore groups attached to the ligand, such as π→π* transitions in double bonds or conjugated systems. At this peak, electrons in the π orbital are excited to the higher-energy π* antibonding orbital. Studies on metal dithiocarbamate complexes support this interpretation, where π→π* transitions typically appear within this wavelength range [20]. The peaks at 274 and 284 nm indicate π→π* or n→π* electronic transitions. In π→π* transitions, electrons from the π orbital are excited to the π* antibonding orbital. In contrast, in n→π* transitions, electrons from non-bonding orbitals (n), such as in carbonyl groups or heteroatom groups (like sulfur), are excited to the π* antibonding orbital. Research on cobalt(III) dithiocarbamate complexes has demonstrated absorption bands in the ultraviolet region associated with these transitions [21]. Furthermore, the 294 and 305 nm peaks suggest the possibility of d-d transitions or Ligand-to-Metal Charge Transfer (LMCT). In d-d transitions, electrons in the d orbitals of the Mn(II) metal transfer between different energy levels within the split d orbitals due to the ligand field. In contrast, LMCT transitions involve the excitation of electrons from ligand orbitals to higher-energy metal orbitals. Similar phenomena have been reported in the Mn(II) cysteine-alanine dithiocarbamate complex [15]

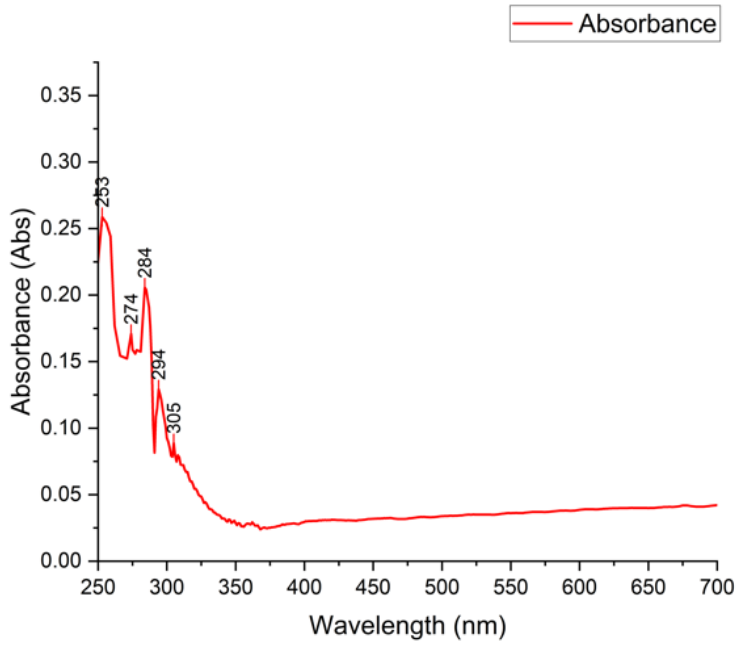

Figure 4 *UV-Vis absorption spectrum of Mn(II) Cys-Ala Dithiocarbamate complex in ethanol, indicating π→π*, n→π**, and potential d–d or LMCT transitions relevant to ligand-metal coordination and electronic structure.

IR characterization

The Mn(II) Cysteine-Alanine dipeptide dithiocarbamate molecule showed clear absorption peaks connected to different functional groups in FTIR spectroscopy (**Figure 5**). The peak at 3338.78 cm^{-1} could mean that the amide group is stretching or that there is a hydroxyl group (-OH) because the carboxylate group is vibrating in an uneven way. This finding backs up what another study found: strong peaks in the 3000 - 3500 cm^{-1} range mean that hydroxyl groups are present [22].

The peak at 2918.30 cm^{-1} shows aliphatic C-H stretching from alkane chains. This is supported by studies that show sharp peaks at 2943.42 and 2975.29 cm^{-1}, along with different stretching vibrations, show C-H bonds in CH_3 groups. [23]. In the wavenumber region of 1597.06 cm^{-1} and 1408.04 cm^{-1}, firm absorption peaks suggest the presence of C=O stretching in carbonyl groups and asymmetric vibrations of carboxylate groups ($-COO^-$), characteristic of peptide compounds. This observation is supported by studies reporting that carbonyl and carboxylate groups exhibit significant peaks within the 1500 - 2000 cm^{-1} range [24].

Additional peaks at 1238.09 and 1253.73 cm^{-1} indicate C-N vibrations from the amide group, consistent with reports that C-N vibrations typically occur in the 1250 - 1350 cm^{-1} range [25]. Furthermore, peaks at 572.28 cm^{-1} and 689.30 cm^{-1} support C-S stretching associated with dithiocarbamate components, which fall within the 570 - 705 cm^{-1} range [20]. Lastly, peaks at 1130.29 and 1053.92 cm^{-1} suggest the possibility of C-O stretching from alcohol or ester groups, as identified in other studies indicating that these stretches are typically found in dipeptide molecular complexes within the 1100 - 1150 cm^{-1} range [20].

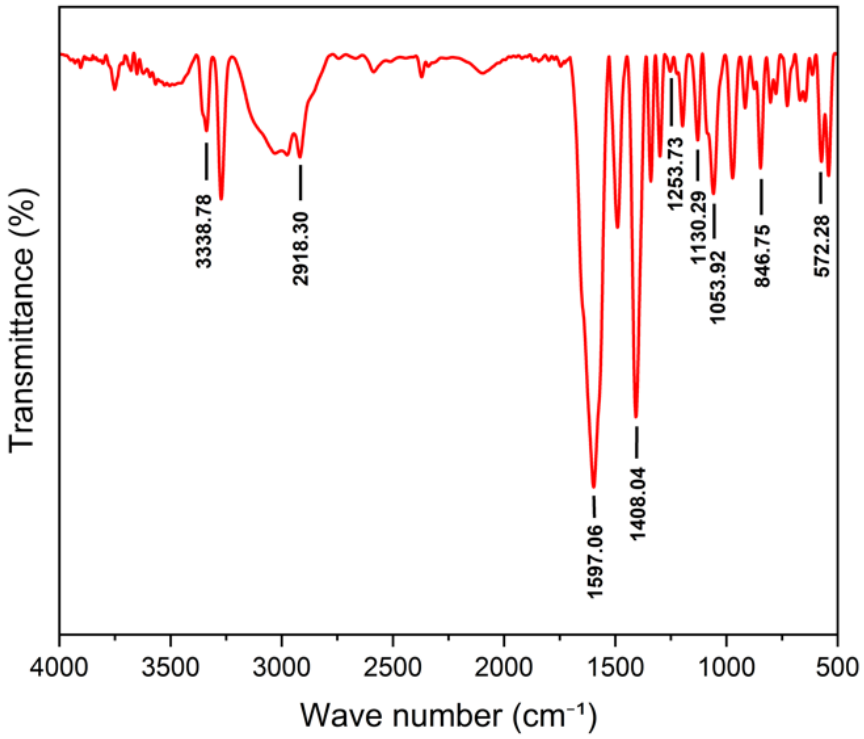

Figure 5 FTIR spectrum of the Mn(II) Cys-Ala Dithiocarbamate complex showing characteristic vibrational bands (e.g., NH, C=O, CS_2), supporting the presence of peptide and dithiocarbamate coordination groups.

XRD characterization

According to **Figure 6**, the XRD analysis of the Mn(II) Cysteine-Alanine Dipeptide Dithiocarbamate compound reveals the presence of a crystalline structure characterized by prominent diffraction peaks at $2\theta \approx 28°$, 32°, 43° and 60°. These peaks exhibit sharp intensities, indicating high crystallinity and molecular structural order. The observed peaks were indexed using

POWDER X software [26]. Miller indices such as 010, 110, and 020 were assigned, representing specific crystalline planes contributing to the diffraction pattern. This observation is further supported by the fact that these Miller indices correspond to distinct crystalline planes responsible for the diffraction pattern. Moreover, the symmetry and order suggested by the diffraction pattern strongly indicate that the compound likely possesses an orthorhombic or tetragonal crystal system [27].

Lattice parameter calculations using Bragg's law and the orthorhombic crystal system equation yielded approximate values of a = 3.40 Å and b = 2.48 Å, further supporting the assignment of orthorhombic symmetry. Since all indexed planes involve only the h and k components with l = 0, the calculations were restricted to the a and b lattice parameters. However, due to the absence of higher-order reflections involving the c-axis, the full 3-dimensional lattice could not be resolved, and the possibility of tetragonal symmetry cannot be completely ruled out. This limitation is common when dealing with powder X-ray diffraction data that predominantly reflects planes parallel to the sample surface or with preferred orientations [28]. Therefore, further structural refinement using advanced techniques such as Rietveld or single-crystal XRD is essential to unambiguously determining the complete crystal system and atomic arrangement. The Rietveld method, in particular, provides powerful tools for modeling entire diffraction patterns and refining crystal structure parameters from powder data with high precision [29]

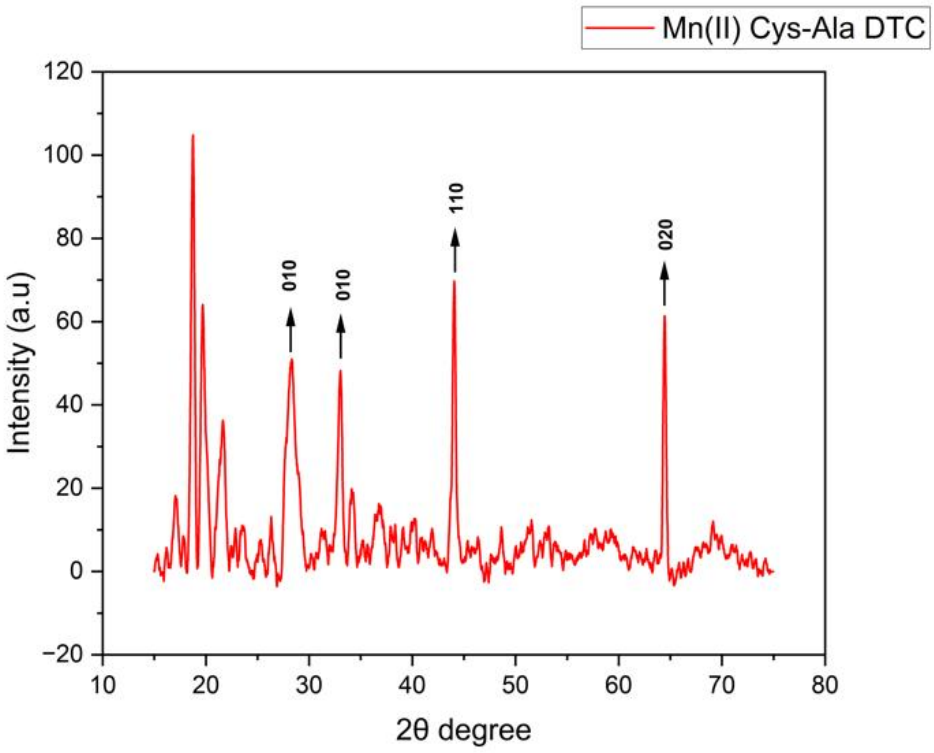

Figure 6 XRD diffractogram indicating crystalline nature of Mn(II) Cys-Ala Dithiocarbamate complex with distinct peaks corresponding to orthorhombic/tetragonal symmetry and lattice parameters, confirming structural order.

SEM characterization

Based on **Figure 7**, the SEM (Scanning Electron Microscope) analysis of the Mn(II) Cysteine-Alanine Dipeptide Dithiocarbamate compound reveals that the particle morphology exhibits irregular structures with rough and porous surfaces. At a magnification of 2000×, the compound shows a crystalline structure with rod-like or plate-like shapes arranged in an orderly manner. The particle surfaces appear rough, with numerous small aggregate-like structures adhering to the rods or plates. This suggests the possibility of effective crystalline nucleation during the compound's formation [30].

The scale bar in the image indicates that the particle size ranges from 2 to 8 μm, with smaller particles dispersed and attached to larger structures. The layered structure suggests the presence of semi-crystalline crystals, which are commonly formed in metal-peptide complex compounds. These smaller particles could be associated with the aggregation of secondary crystals or aggregation processes occurring during synthesis [31]

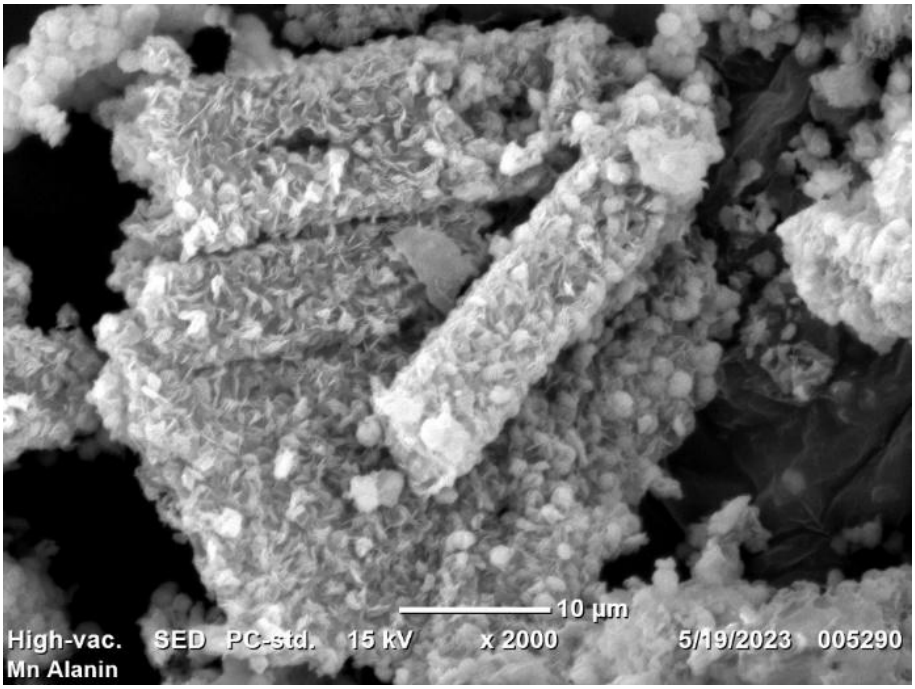

Figure 7 SEM micrograph of Mn(II) Cys-Ala Dithiocarbamate complex revealing porous and irregular particle morphology, suggesting semi-crystalline nature and effective nucleation during synthesis.

SEM-EDS characterization

The EDS analysis of the Mn(II) Cysteine-Alanine Dipeptide Dithiocarbamate compound reveals the primary elemental composition, with sulfur (S) accounting for 55.48% by mass, manganese (Mn) at 35.64% by mass and smaller amounts of carbon (C), nitrogen (N), and oxygen (O), at 0.85, 1.28 and 6.75% by mass, respectively (**Figure 8**). The high sulfur content highlights the dominance of the dithiocarbamate (-CS_2) group in the compound's structure. In contrast, the significant manganese content indicates the presence of Mn(II) ions as the metal centre in the complex. A study by Martini *et al.* [25] reported similar findings in Mn(II)-dithiocarbamate complexes, where sulfur and manganese were the dominant elements in the structure [25]. This is consistent with the results of Zare *et al.* [34], who found that Mn(II) Schiff base complexes' porous structure performed exceptionally well as functional materials in catalytic processes [32]

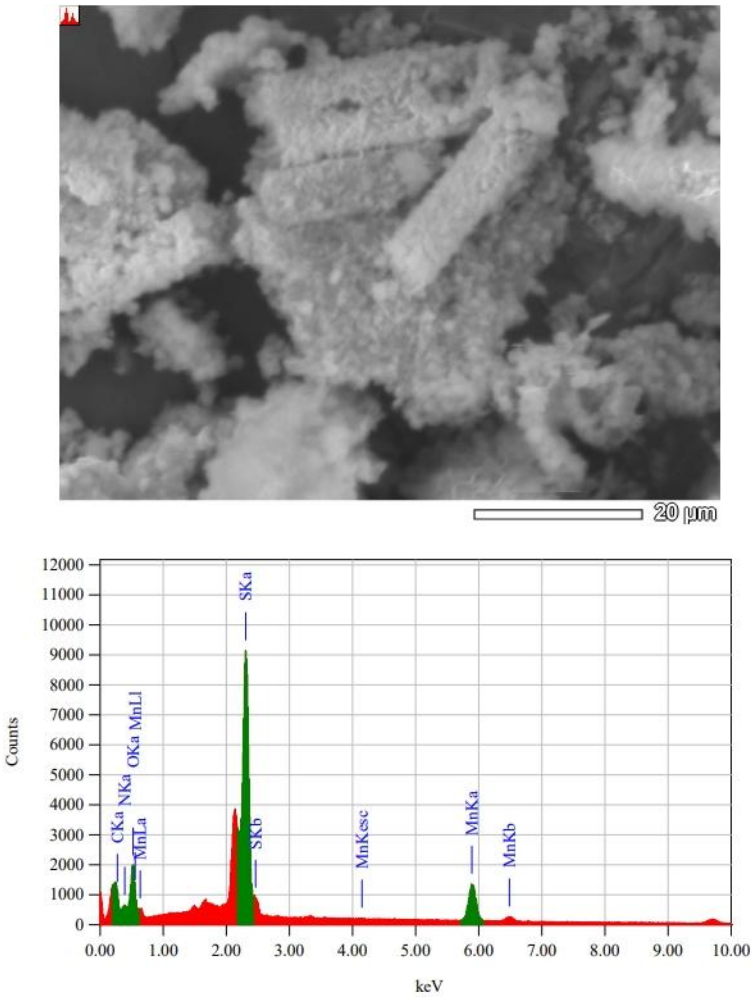

Figure 8 SEM-EDS analysis of Mn(II) Cys-Ala Dithiocarbamate complex highlighting surface morphology and elemental composition, confirming the dominance of Mn and S, consistent with dithiocarbamate-based coordination.

Cytotoxicity of Mn(II) complexes derived from cysteine-alanine dithiocarbamate on the MCF-7 breast cancer cell line

We performed the cytotoxicity assay using the MTS method (3-(4,5-dimethylthiazol-2-yl)-5-(3-carboxymethoxyphenyl)-2-(4-sulfophenyl)-2H-tetrazolium). This method was selected due to its prominence as a widely utilized approach for assessing cytotoxicity and cell proliferation *in vitro*, as stipulated by the research protocol from [33]. This method can provide accurate results regarding cell viability measurement after exposure to chemical compounds.

To ensure the reliability of the results, positive and negative controls were included in the assay. Cisplatin was used as the positive control, as it is a standard chemotherapeutic agent known for its cytotoxic effects against cancer cells, including MCF-7. As shown in **Figures 9** and **10**, treatment with Cisplatin resulted in a bluish-purple color and evident morphological changes, such as cell shrinkage and loss of adherence, indicating decreased cell viability. This finding is supported by a study that reported Cisplatin could reduce MCF-7 cell viability with an IC_{50} value of 5.7 µg/mL [34]. On the other hand, the negative control in this study was 2% DMSO, the solvent used to dissolve the test compound. The DMSO control exhibited no significant toxic effect, as indicated by the bright pink coloration and the presence of healthy, confluent cells under the microscope. This suggests that the solvent itself did not interfere with cell viability. However, several studies have reported that DMSO began to show significant toxicity at concentrations above 0.5% against MCF-7

cells [35], and could even inhibit the proliferation of mouse breast cancer cells more strongly than thalidomide [36]. Therefore, its concentration must be carefully optimized to avoid misinterpreting the compound's cytotoxic effects. These controls validated the assay by demonstrating that the observed cytotoxicity was attributable to the Mn(II) complex, not the solvent or culture conditions.

The cytotoxicity testing of the Mn(II)-based cysteine-alanine dithiocarbamate complex demonstrated a dose-dependent toxic effect on the test cells. Based on the documentation on the well plate (**Figure 9**), a colour change in the medium from blue to pink indicated a reduction in cell viability. The higher the concentration of Mn-alanine, the more pronounced the colour change, reflecting a decrease in cellular metabolic activity, likely indicative of its cytotoxic effects, as confirmed by cellular microscopy (**Figure 10**). These findings are consistent with previous studies showing that higher concentrations of cytotoxic compounds result in lower cell viability, as evidenced by a decrease in colour intensity [37]

Media	Media + Cell	Cisplatin	Solvent	Sample Concentration (µg/mL)							
				7,81	15,63	31,25	62,50	125,00	250,00	500,00	1000,00

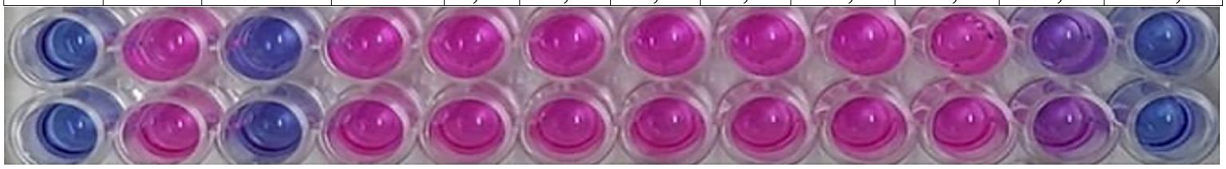

Figure 8 Well plate images from cytotoxicity assay showing colorimetric changes in PrestoBlue reagent, illustrating dose-dependent reduction in MCF-7 cell viability by the Mn(II) Cys-Ala complex.

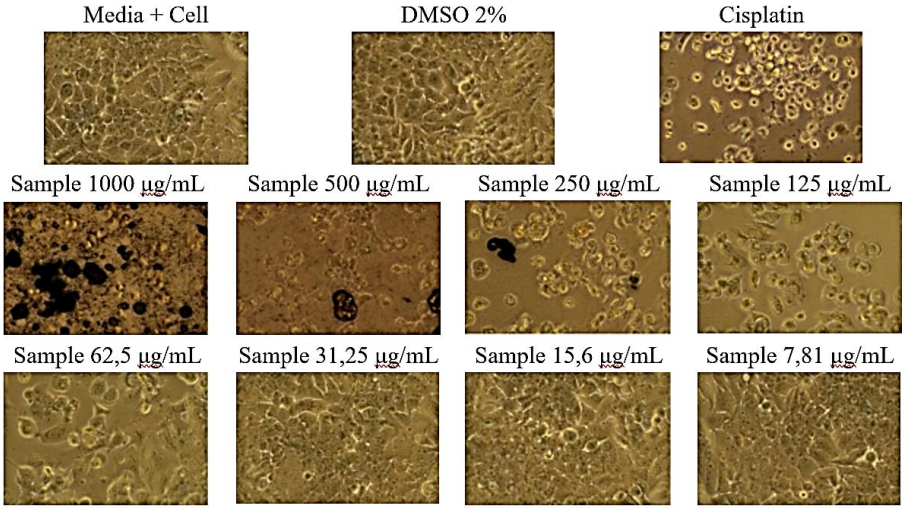

Figure 9 Microscopic observation of MCF-7 cells after treatment with Mn(II) Cys-Ala complex, showing apoptotic features such as shrinkage and detachment, indicating induced cell death.

Each concentration of the Mn(II)-alanine complex was tested on MCF-7 cells in 2 independent replicates to ensure data reproducibility. Cell viability data were analyzed using one-way ANOVA, revealing a highly significant difference between treatment groups ($F = 50446.40$; $p < 0.0001$), far exceeding the critical F value (3.50). This result indicates that increasing the concentration of the Mn(II)-alanine complex significantly reduced cell viability. Post hoc analysis using a 2-sample t-test with unequal variances and Bonferroni correction ($\alpha = 0.00625$) confirmed that all concentrations from 7.81 to 1000 µg/mL were significantly different from the control group ($p < 0.005$), demonstrating a concentration-dependent cytotoxic effect.

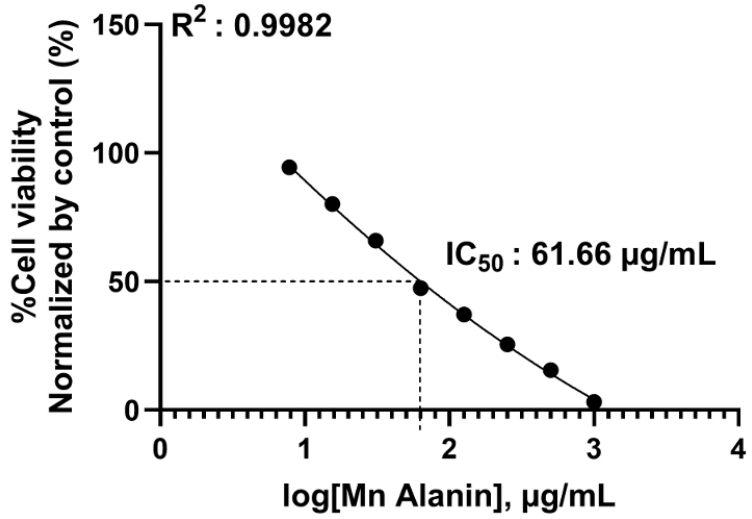

Figure 10 Dose-response curve of Mn(II) Cys-Ala complex on MCF-7 cell viability, indicating IC50 value of 61.66 µg/mL with a sigmoidal trend, reflecting concentration-dependent cytotoxicity.

Based on **Figure 11**, The IC_{50} value, calculated through nonlinear sigmoid curve fitting using GraphPad Prism, was 61.66 µg/mL (R^2 = 0.9982), indicating excellent model fitting. Morphological observations supported the quantitative results: at higher concentrations (≥ 250 µg/mL), cells exhibited visible signs of cytotoxicity, such as aggregation and apoptotic features. At lower concentrations (7.81 - 62.50 µg/mL), cells maintained relatively normal morphology, though minor indications of cellular stress were observed.

These findings indicate that the Mn(II)-alanine complex effectively inhibits 50% of MCF-7 cell viability at moderate concentrations and exerts increasing cytotoxic effects with concentration. This is in agreement with previous studies on Mn(II) complexes containing arginine-derived dithiocarbamates, which showed IC_{50} values of 211.53 µg/mL against MCF-7 cells, along with notable morphological damage [34].

Furthermore, the Mn(II)-emodin complex demonstrated a 2 to 3 fold decrease in IC_{50} compared to free emodin and cisplatin across various cancer cell lines, including MCF-7. The IC_{50} values recorded were 54.61 ± 0.33 µg/mL at 24 h, 27.43 ± 0.47 µg/mL at 48 h, and 4.90 ± 0.28 µg/mL at 72 h, indicating a time-dependent enhancement of cytotoxic effects [38]. In addition, the β-diiminato manganese(III) complex significantly reduced cell viability in a dose-dependent manner in both MCF-7 and MDA-MB-231 cells. The IC_{50} values were 1.44 ± 0.24 µg/mL (2.8 ± 0.47 µM) for MCF-7 and 2.28 ± 0.38 µg/mL (4.4 ± 0.75 µM) after 24 h of treatment. The mechanism of action involved cell cycle arrest and intrinsic apoptotic cell death, suggesting a strong potential for development as a transition metal-based chemotherapeutic agent [39].

Conclusions

The characterization results indicate that the Mn(II) cysteine-alanine dithiocarbamate complex exhibits high thermal stability and weak electrolytic properties, with an electrical conductivity of 1.5 mS/cm at 28 °C. This stability is attributed to the strong interactions between the Mn(II) ion and the organic ligand. Docking analysis reveals that the complex interacts with the estrogen receptor α through various mechanisms, including hydrogen bonding and van der Waals interactions, ensuring stability at the protein's active site. Compared to the control molecule, the complex demonstrates more diverse and specific interaction patterns.

UV-Vis and IR spectroscopy characterizations reveal electronic transitions relevant to the complex's structure, such as π→π* and d-d transitions, as well as characteristic functional group vibrations, including -NH, $-COO^-$, and $-CS_2$. The XRD diffraction pattern confirms an ordered crystal structure, while SEM analysis shows irregular particle morphology with a

porous surface, supporting the formation of semi-ordered crystals. Cytotoxicity tests on MCF-7 breast cancer cells demonstrate dose-dependent toxic effects, with an IC_{50} value of 61.66 µg/mL. This confirms the potential of this complex as an anticancer agent, comparable to or better than similar complexes previously reported.

However, this study has not yet evaluated the compound's selectivity toward non-cancerous normal cells, which is a critical parameter for assessing clinical potential. Therefore, further studies are needed to examine the cytotoxic effects on healthy cells such as fibroblasts or normal epithelial cells. Suppose the compound is shown to be non-selective. In that case, further initiatives may include modifying ligand structures or integrating them into tailored drug delivery systems to improve efficacy and minimize systemic toxicity.

Acknowledgements

We sincerely thank the Central Laboratory for Inorganic and Organic Research, the Integrated Chemistry Laboratory, and the Science Research and Development Laboratory for their invaluable research support. We also extend our gratitude to Hasanuddin University, Makassar, Indonesia, for providing the necessary facilities and resources that contributed to the success of this study.

Declaration of Generative AI in Scientific Writing

- This manuscript utilized generative AI tools, namely ChatGPT (OpenAI) and Grammarly, to enhance language clarity, grammar, and overall readability.
- All AI-assisted edits were made under strict human oversight and control.
- These tools were not used to:
  - Generate scientific content.
  - Interpret or analyze data.
  - Develop research questions.
  - Draw or formulate conclusions.
- The authors are responsible for the manuscript's intellectual content, scientific accuracy, and integrity.

CRediT author statement

Andi Besse Khaerunisa: Conceptualization, Methodology, Writing – Original Draft, Visualization. **Indah Raya:** Supervision, Project Administration, Writing – Review & Editing, Funding Acquisition. **Hasnah Natsir:** Investigation, Resources, Writing – Review & Editing. **Nunuk Hariani Soekamto:** Validation, Formal Analysis, Writing – Review & Editing. **Abdul Wahid Wahab:** Methodology, Software, Data Curation. **Rugaiyah Arfah:** Investigation, Resources. **Rizal Irfandi:** Software, Formal Analysis, Visualization. **Eka Pratiwi:** Data Curation, Investigation. **Wahyudin Rauf:** Writing – Review & Editing, Validation. **Andi Adillah Nur Syafirah:** Software, Visualization.

References

[1] L Lv, S Yang, Y Zhu, X Zhai, S Li, X Tao and D Dong. Relationship between metabolic reprogramming and drug resistance in breast cancer. *Frontiers in Oncology* 2022; **12**, 942064.

[2] SS Said and WN Ibrahim. Cancer Resistance to Immunotherapy: Comprehensive Insights with Future Perspectives. *Pharmaceutics* 2023; **15(4)**, 1143.

[3] ST Wong and S Goodin. Overcoming drug resistance in patients with metastatic breast cancer. *Pharmacotherapy: The Journal of Human Pharmacology and Drug Therapy* 2012; **29(8)**, 954-965.

[4] WS Dalton. Mechanisms of drug resistance in breast cancer. *Seminars in Oncology* 1990; **17(4S 7)**, 37-39.

[5] M Xiao, J He, L Yin, X Chen, X Zu and Y Shen. Tumor-Associated macrophages: Critical players in drug resistance of breast cancer. *Frontiers in Immunology* 2021; **12**, 799428.

[6] B Biersack, A Ahmad, FH Sarkar and R Schobert. Coinage metal complexes against breast cancer. *Current Medicinal Chemistry* 2012; **19(23)**, 3949-3956.

[7] P Zhang and PJ Sadler. Redox-active metal complexes for anticancer therapy. *European Journal of Inorganic Chemistry* 2017; **2017(12)**, 1541-1548.

[8] EJ Martinez-Finley, CE Gavin, M Aschner and TE Gunter. Manganese neurotoxicity and the role of

reactive oxygen species. *Free Radical Biology and Medicine* 2013; **62**, 65-75.

[9] S Yadamani, A Neamati, M Homayouni-Tabrizi, SA Beyramabadi, S Yadamani, A Gharib, A Morsali and M Khashi. Treatment of the breast cancer by using low frequency electromagnetic fields and Mn(II) complex of a Schiff base derived from the pyridoxal. *The Breast* 2018; **41**, 107-112.

[10] Y Wang, D Zhong, F Xie, S Chen, Z Ma, X Yang, MZ Iqbal, Q Zhang, J Lu, S Wang, R Zhao and X Kong. Manganese phosphate-doxorubicin-based nanomedicines using mimetic mineralization for cancer chemotherapy. *ACS Biomaterials Science & Engineering* 2022; **8(5)**, 1930-1941.

[11] JO Adeyemi and DC Onwudiwe. The mechanisms of action involving dithiocarbamate complexes in biological systems. *Inorganica Chimica Acta* 2020; **511**, 119809.

[12] H Tang, D Chen, C Li, C Zheng, X Wu, Y Zhang, Q Song and W Fei. Dual GSH-exhausting sorafenib loaded manganese-silica nanodrugs for inducing the ferroptosis of hepatocellular carcinoma cells. *International Journal of Pharmaceutics* 2019; **572**, 118782.

[13] N Pothayee, N Pothayee, N Hu, R Zhang, DF Kelly, AP Koretsky and JS Riffle. Manganese graft ionomer complexes (MaGICs) for dual imaging and chemotherapy. *Journal of Materials Chemistry B* 2014; **2(8)**, 1087-1099.

[14] EP Istyastono. Docking studies of curcumin as a potential lead compound to develop novel dipeptydyl peptidase-4 inhibitors. *Indonesian Journal of Chemistry* 2010; **9(1)**, 132-136.

[15] RA Arfah, E Pratiwi, I Raya, H Natsir, P Taba, H Rasyid, M Alfliadhi, AB Khaerunnisa, R Irfandi and S Jarre. Design, synthesis and characterization of Mn(II)cysteine-tyrosine dithiocarbamate complex for against the cancer on MCF-7 breast cancer cell line. *Asian Pacific Journal of Cancer Prevention* 2024; **25(9)**, 3251-3261.

[16] S Jarre, I Raya, Prihantono and S Santi. Synthesis, characterization, molecular docking studies of Mn(II)Prolinedithiocarbamate and its potential as anticancer agents. *Molecular Diversity* 2024; **28(2)**, 889-900.

[17] M Remelli, M Peana, S Medici, M Ostrowska, E Gumienna-Kontecka and MA Zoroddu. Manganism and parkinson's disease: Mn(II) and Zn(II) interaction with a 30-amino acid fragment. *Dalton Transactions* 2016; **45(12)**, 5151-5161.

[18] L Gao, Y Tu, P Wegman, S Wingren and LA Eriksson. Conformational enantiomerization and estrogen receptor α binding of anti-cancer drug tamoxifen and its derivatives. *Journal of Chemical Information and Modeling* 2011; **51(2)**, 306-314.

[19] R Ugarte. *FMO study of the interaction energy between human estrogen receptor alpha and selected ligands*. arXiv, New York, 2022.

[20] DC Onwudiwe and AC Ekennia. Synthesis, characterization, thermal, antimicrobial and antioxidant studies of some transition metal dithiocarbamates. *Research on Chemical Intermediates* 2017; **43(3)**, 1465-1485.

[21] G Gurumoorthy. Synthesis and characterization of cobalt(III) dithiocarbamate complexes. *International Journal of Modern Agriculture* 2020; **9(4)**, 2200-2203.

[22] ABD Nandiyanto, R Ragadhita and M Fiandini. Interpretation of fourier transform infrared spectra (FTIR): A practical approach in the polymer/plastic thermal decomposition. *Indonesian Journal of Science and Technology* 2023; **8(1)**, 113-126.

[23] ZP Zhang, MZ Rong, MQ Zhang and C Yuan. Alkoxyamine with reduced homolysis temperature and its application in repeated autonomous self-healing of stiff polymers. *Polymer Chemistry* 2013; **4(17)**, 4648-4654.

[24] A Puspita, S Budi and F Kurniadewi. Sintesis besi bervalensi nol menggunakan polifenol dari ekstrak biji kopi. *Jurnal Riset Sains dan Kimia Terapan* 2019; **8(2)**, 9-15.

[25] P Martini, A Boschi, L Marvelli, L Uccelli, S Carli, G Cruciani, E Marzola, A Fantinati, J Esposito and A Duatti. Synthesis and characterization of manganese dithiocarbamate complexes: New evidence of dioxygen activation. *Molecules* 2021; **26(19)**, 5954.

[26] C Dong. PowderX: Windows-95-based program for powder X-ray diffraction data processing. *Journal of Applied Crystallography* 1999; **32(4)**, 838.

[27] ML Low. *Synthesis, characterization and bioactivites of dithiocarbazate schiff base ligands*

and their metal complexes. Universite Pierre et Marie Curie, Paris, France, 2014.

[28] MA Wahab. *Determination of crystal structure parameters.* Springer, Singapore, 2021.

[29] D Asmi, P Manurung and IM Low. *Manufacture of graded ceramic matrix composites by infiltration technique*. Woodhead Publishing, Sawston, 2018.

[30] N Nurlia, M Anas and E Erniwati. Analisis variasi temperatur aktivasi terhadap struktur kristalin arang aktif dari tandan aren (arenga pinnata merr) dengan agen aktivasi potassium silicate (K2SiO3). *Jurnal Penelitian Pendidikan Fisika* 2020; **5(4)**, 300.

[31] R Maharani, DY Kurnia, AT Hidayat, J Al-Anshori, D Sumiarsa, D Harneti and N Nurlelasari. Upaya optimasi sintesis pentapeptida Leu-Ala-Asn-Ala-Lys dengan pengurangan nilai loading resin. *Chimica et Natura Acta* 2020; **8(1)**, 26-35.

[32] N Zare, A Zabardasti, A Mohammadi, F Azarbani and A Kakanejadifard. Sonochemical synthesis, characterization, biological applications, and DFT study of new nano-sized manganese complex of azomethine derivative of diaminomaleonitrile. *Journal of the Iranian Chemical Society* 2019; **16(7)**, 1501-1516.

[33] Y Wang, DT Nguyen, G Yang, J Anesi, Z Chai, F Charchar and J Golledge. An improved 3-(4,5-di-methylthiazol-2-yl)-5-(3-carboxymethoxyphenyl) -2-(4-sulfophenyl)-2H-tetrazolium proliferation assay to overcome the interference of hydralazine. *ASSAY and Drug Development Technologies* 2020; **18(8)**, 379-384.

[34] Prihantono, R Irfandi, I Raya and Warsinggih. Potential anticancer activity of Mn (II) complexes containing arginine dithiocarbamate ligand on MCF-7 breast cancer cell lines. *Annals of Medicine and Surgery* 2020; **60**, 396-406.

[35] L Jamalzadeh, H Ghafoori, R Sariri, H Rabuti, J Nasirzade, H Hasani and MR Aghamaali. Cytotoxic effects of some common organic solvents on MCF-7, RAW-264.7 and human umbilical vein endothelial cells. *Avicenna Journal of Medical Biochemistry* 2016; **4(1)**, e33453.

[36] ES Oz, E Aydemir and K Fiskin. DMSO exhibits similar cytotoxicity effects to thalidomide in mouse breast cancer cells. *Oncology Letters* 2012; **3(4)**, 927-929.

[37] K Prabst, H Engelhardt, S Ringgeler and H Hubner. Basic colorimetric proliferation assays: MTT, WST, and Resazurin. *Cell Viability Assays* 2017; **1601**, 1-17.

[38] L Yang, J Tan, B Wang and L Zhu. Synthesis, characterization, and anti-cancer activity of emodin-Mn(II) metal complex. *Chinese Journal of Natural Medicines* 2014; **12(12)**, 937-942.

[39] R Farghadani, J Rajarajeswaran, NB Mohd Hashim, MA Abdulla and S Muniandy. A novel β-diiminato manganese(III) complex as the promising anticancer agent induces G0/G1 cell cycle arrest and triggers apoptosis via mitochondrial-dependent pathways in MCF-7 and MDA-MB-231 human breast cancer cells. *RSC Advances* 2017; **7(39)**, 24387-24398.